Integrative analysis of exosomal microRNA-149-5p in lung adenocarcinoma

Wen Tian
Chinese Academy of Medical Sciences and Peking Union Medical College
He Yang
Chinese Academy of Medical Sciences and Peking Union Medical College
Baosen Zhou (bszhou@cmu.edu.cn)
Shengjing Hospital of China Medical University

Research

Keywords: exosomal miR-149-5p, WGCNA, AMOTL2, MSRB3

Posted Date: April 17th, 2020

DOI: https://doi.org/10.21203/rs.3.rs-21762/v1

Version of Record: A version of this preprint was published at Aging on February 26th, 2021. See the published version at https://doi.org/10.18632/aging.202596.

Abstract

Background

Exosomes play an important role in the regulation of various processes in the tumor microenvironment. In this study, we explored the mechanisms of exosomal miR-149-5p in the pathogenesis of lung adenocarcinoma.

Methods

Raw GEO data were downloaded and normalized using the R package. Exosomal miRNAs that were found to be significantly expressed were subjected to WGCNA co-expression network analysis. The proliferation, migration and apoptotic abilities of tumor cells were assessed by the MTS, Transwell and apoptosis assays. Univariate and multivariate analyses were performed to identify the independent factors of target genes.

Results

Results showed that exosomal miR-149-5p was enriched in peripheral serum and tumor cells. The upregulation of exosomal miR-149-5p promoted the growth and migration of tumor cells, and inhibited apoptosis of tumor cells. Notably, target genes of exosomal miR-149-5p, AMOTL2 and MSRB3, were significantly downregulated in lung adenocarcinoma and thus may be considered as independent risk factors of poor survival. In TCGA-LUAD cohort, miR-149-5p was found to be a negative regulator of AMOTL2 and MSRB3 genes.

Conclusion

Collectively, these results provide novel insights for further mechanistic studies on lung adenocarcinoma.

Background

Lung cancer is the leading cause of cancer-related deaths in the world[1]. In China, an estimated 733,300 new lung cancer cases and 610,200 lung cancer deaths were recorded in 2015[2]. Lung adenocarcinoma is a complicated subtype of lung cancer[3]. Numerous studies have explored the molecular mechanisms of this cancer[4–6]. In our study, we investigated its pathomechanism to provide novel diagnostic and therapeutic biomarkers in lung adenocarcinoma.

Exosomes are endosomes-derived vesicles with the sizes in the range of 40-150nm[7]. They transport RNAs and proteins to recipient cells[8], and regulate tumor microenvironment[9–11]. In breast cancer, it was found that MDA-MB-231 cells released exosomes containing miR-10b. The exosomal miR-10b suppressed the invasion ability of HMLE cells[12]. Elsewhere, exosomal miR-382-5p released from oral squamous cell carcinoma cells stimulated tumor cells migration and invasion ability[13].

In previous studies, miR-149-5p was found to be highly expressed in lung adenocarcinoma cells and influenced tumor cells metastasis[14, 15]. However, the roles of exosomal miR-149-5p remain unclear. In this study, we constructed a WGCNA co-expression network to identify the key exosomal miRNA from GEO dataset. Moreover, we explored the effect of exosomal miR-149-5p on tumor cells proliferation, migration and apoptosis. Our results showed that target genes of exosomal miR-149-5p were significantly associated with poor survival of lung adenocarcinoma patients.

Methods

Raw data collection

Raw data were downloaded from GEO and normalized using the R software. GSE111803 contained 5 lung adenocarcinoma patients and 5 healthy controls. Adjusted $p < 0.05$ and $|\log_2 FC|>1$ were set as the criterion for differently expressed exosomal miRNAs. Raw count data and clinical characteristics of TCGA-LUAD cohort were downloaded using the R TCGAbiolinks package.

Construction of WGCNA co-expression network

WGCNA co-expression network was constructed via the R WGCNA package. Exosomal miRNAs were classified into different modules. The soft threshold was calculated when scale-free $R^2 > 0.9$. Then the cluster dendrogram and network heatmap of selected miRNAs were executed. Eigengene values of modules were calculated and the eigengene adjacency heatmap was carried out.

Pathway prediction

DIANA-miRPath provides miRNA pathway analyses and accurate statistics. Pathways of exosomal miRNAs in each module were predicted.

Exosomes isolation and identification

Exosomes were isolated by Minute™ Hi-Efficiency Exosome Precipitation Reagent (Invent EI-027) according to the protocol and then filtered with a 0.22 μm filter to purify the exosomes. The exosomes were identified by transmission electron microscope observation and exosomal protein biomarkers. The exosomes were fixed with 4% glutaraldehyde at 4℃ for 2 h, and then rinsed three times with 0.1 mol/L PBS and fixed with 1% osmium tetroxide for 2 h. Next, dehydrated by conventional ethanol and gradient acetone, exosomes were immersed, embedded, polymerized in epoxy resin and then observed under a transmission electron microscope. The proteins from exosomes were lysed with cell lysis buffer (Takara 635656). CD63 (Abcam 125011) and TSG101 (Abcam 134045) were used as exosome markers.

Cells culture

HBE and A549 cells were cultured in RPMI 1640 media at 37℃ with 5% CO_2.

RNA isolation and RT-PCR

Total RNA was isolated by RNAiso Plus (TAKARA 9108). Reverse transfection was conducted according to the TAKARA 638313 kit manufacturer`s instructions. And then RT-PCR was performted using TAKARA RR820A kit.

Cells transfection

A549 cells were divided into four groups: blank, miR-149-5p-mimic, miR-149-5p-inhibitor and NC. Plasmids were designed from Syngeneiech (Beijing, China). $1*10^5$ cells were seeded into 6-well plates and transfected plasmids using jetPRIME transfection reagent (Ploylus transfection). After transfection 24 hours, cells were collected for the following experiments.

Cells proliferation assays

Cells proliferation was tested using MTS (Promega G3580) according to manufacturer`s instructions. $5*10^3$ cells were seeded into 96-well plates and cultured for 0–72 h. 20μL MTS solution was added into each well and incubated for 3 h at 37℃ with 5%CO_2. The OD was measured at 490 nm.

Cells migration assays

$2*10^5$ cells with serum-free medium were seeded into apical chambers of 24-well plates and 500μL medium containing 10% FBS was added into basolateral chambers and incubated at 37℃ with 5%CO_2 for 48 h. Then apical chambers were washed with PBS twice and immersed in methanol for 20 min. Next the apical chambers washed with PBS twice were stained with 0.1% crystal violet for 8 min. The cells were observed using an inverted fluorescence microscope. Each experiment was repeated three times.

Cells apoptosis assays

The cells were harvested when they reached 80% confluence and washed with PBS twice. Annexin V-APC/7-AAD kit (KeyGEN BioTECH KGA1023) was used to test treated cells apoptosis according to manufacturer`s instructions. The percentage of apoptotic cells were assayed by flow cytometry.

Identification of candidate genes of exosomal miR-149-5p

Targetscan, miRWalk, miRDB and miRDIP bioinformatic websites were performed to predict the targeted genes of exosomal miR-149-5p. Kaplan-Meier Plotter was used to assess the overall survival of targeted genes in lung adenocarcinoma.

Statistics analysis

Differences between two groups were compared using T-test. Differences among multiple groups were compared using one-way analysis of variance. Univariate and multivariate analyses were performed by SPSS 20.0. A value of $p < 0.05$ was considered to be statistically significant.

Results

Differently expressed exosomal miRNAs in GSE111803

Normalized data for each group in GSE111803 was showed in Fig. 1A. The result plotted the similar expression distribution in each group. According to the criterion of adjusted $p < 0.05$ and $|log2FC|>1$, a total of 559 miRNAs were identified. Among them, 36 significantly expressed exosomal miRNAs were displayed in the heat map (Fig. 1B).

WGCNA co-expression network of exosomal miRNAs

The power of $\beta = 12$ was chosen as the soft thresholding power value when the scale free $R^2 > 0.95$ (Fig. 2A). A total of 10 modules were identified (Fig. 2B). Each module had different numbers of exosomal miRNAs (Table 1). The modules were highly independent of each other (Fig. 2C). In addition, to explore co-expression similarity of each module, we calculated the eigengenes based on their correlation (Fig. 2D). These ten modules yielded two main clusters; one contained six modules, while the other contained four modules. The heatmap plot of the adjacencies also supported this result (Fig. 2E). Furthermore, we explored the relation between ten modules and lung adenocarcinoma (Table 2). The results showed that the turquoise module had the strongest connection ($P < 0.001$) with NSCLC (hsa05223). In turquoise module, we found that the function of exosomal miR-149-5p in lung adenocarcinoma remained unclear. Thus, we investigated the role of exosomal miR-149-5p for the following experiment.

Table 1
Numbers of exosomal miRNAs in each module

Color	Number	Color	Number
Black	49	Pink	43
Blue	72	Purple	23
Brown	71	Red	61
Green	65	Turquoise	75
Magenta	31	Yellow	69

Table 2

Pathways of exosomal miRNAs in each module

Color	Pathways	*P* value	Color	Pathways	*P* value
Black	Pathways in cancer (hsa05200)	1.419568e-12	Blue	PI3K-Akt signaling pathway (hsa04151)	1.102411e-10
	Bladder cancer (hsa05219)	1.95996e-11		Pathways in cancer (hsa05200)	1.922688e-10
	Pancreatic cancer (hsa05212)	7.393284e-10		ErbB signaling pathway(hsa04012)	1.089081e-09
	PI3K-Akt signaling pathway (hsa04151)	1.277962e-09		MAPK signaling pathway (hsa04010)	6.162801e-09
	Cell cycle (hsa04110)	1.669804e-07		**NSCLC (hsa05223)**	**1.646353e-07**
Brown	ErbB signaling pathway (hsa04012)	1.015039e-24	Green	MAPK signaling pathway (hsa04010)	2.040638e-19
	Neurotrophin signaling pathway (hsa04722)	1.068046e-24		Wnt signaling pathway (hsa04310)	6.65386e-16
	PI3K-Akt signaling pathway (hsa04151)	4.017153e-19		ErbB signaling pathway (hsa04012)	1.039351e-11
	Colorectal cancer (hsa05210)	1.259041e-18		Transcriptional misregulation in cancer (hsa05202)	3.932956e-10
	Wnt signaling pathway (hsa04310)	1.169783e-17		Pathways in cancer (hsa05200)	1.366175e-09
Magenta	Transcriptional misregulation in cancer (hsa05202)	3.953364e-17	Pink	Glutamatergic synapse (hsa04724)	4.911598e-11
	Focal adhesion (hsa04510)	1.703439e-16		Wnt signaling pathway (hsa04310)	1.523735e-10
	ErbB signaling pathway (hsa04012)	8.688603e-15		Neurotrophin signaling pathway (hsa04722)	6.150503e-09
	T cell receptor signaling pathway (hsa04660)	1.116865e-14		MAPK signaling pathway (hsa04010)2.41413e-08	2.41413e-08
	PI3K-Akt signaling pathway (hsa04151)	3.05292e-12		ErbB signaling pathway (hsa04012)	2.639617e-07
Purple	Ubiquitin mediated proteolysis (hsa04120)	1.233083e-12	Red	mTOR signaling pathway (hsa04150)	2.480427e-18

Color	Pathways	*P* value	Color	Pathways	*P* value
	Prion diseases (hsa05020)	8.092908e-12		Prostate cancer (hsa05215)	1.006374e-17
	Colorectal cancer (hsa05210)	8.092908e-12		Pathways in cancer (hsa05200)	1.051852e-16
	Focal adhesion (hsa04510)	1.271225e-11		PI3K-Akt signaling pathway (hsa04151)	1.836449e-16
	TGF-beta signaling pathway (hsa04350)	3.088237e-09		ErbB signaling pathway (hsa04012)	3.106143e-15
Turquoise	mTOR signaling pathway (hsa04150)	2.480427e-18	Yellow	mTOR signaling pathway (hsa04150)	2.480427e-18
	NSCLC (hsa05223)	1.006374e-17		Prostate cancer (hsa05215)	1.006374e-17
	Pathways in cancer (hsa05200)	1.051852e-16		Pathways in cancer (hsa05200)	1.051852e-16
	PI3K-Akt signaling pathway (hsa04151)	1.836449e-16		PI3K-Akt signaling pathway (hsa04151)	1.836449e-16
	ErbB signaling pathway (hsa04012)	3.106143e-15		**NSCLC (hsa05223)**	6.148222e-15

Exosomal miR-149-5p promoted lung adenocarcinoma cells proliferation and migration

Firstly, we found the upregulation of exosomal miR-149-5p in peripheral serum of lung adenocarcinoma patients (Fig. 3A). Then we isolated exosomes from conditioned media and identified the cup-shaped structed and size by electron microscopy (Fig. 3B). In addition, we detected the known exosome biomarkers, CD63 and TSG101 (Fig. 3C). The results verified that the isolated particles were exosomes.

To explore the effect of exosomal miR-149-5p on lung adenocarcinoma tumor cells, we firstly profiled the expression secreted from HBE and A549 cells. Exosomal miR-149-5p was significantly up-regulated in A549 cells compared to HBE cells (Fig. 3D). Then we transfected miR-149-5p-mimic, miR-149-5p-inhibitor and NC into A549 cells. We found a 30-fold increase of miR-149-5p in cells transfected with miR-149-5p-mimic compared to NC (Fig. 3E). A 3-fold decrease of miR-149-5p in cells transfected with miR-149-5p-inhibitor was detected. Next, we measured the expression of exosomal miR-149-5p in different groups. The RT-PCR assays results revealed the over-expression of exosomal miR-149-5p in miR-149-5p-mimic cells by over 7-fold and low-expression in miR-149-5p-inhibitor cells by over 2-fold compared to the NC (Fig. 3F).

As shown in Fig. 3G, MTS assays showed that up-regulation of exosomal miR-149-5p promoted A549 cells proliferation and this function was blocked by exosomal miR-149-5p-inhibitor. The growth rate of

cells transfected with NC was similar to blank group. Additionally, upregulation of exosomal miR-149-5p significantly induced migration ability in A549 cells (Fig. 3H).

Up-regulation of exosomal miR-149-5p suppressed lung adenocarcinoma cells apoptosis

As shown in Fig. 3I, the apoptotic rate of A549 cells transfected with miR-149-5p-inhibitor was significantly higher than cells transfected with NC and miR-149-5p-mimic. Compared to the NC group, the apoptotic rate of the blank group was not significantly changed.

Down-regulation of target genes of exosomal miR-149-5p were associated with survival

We summarized the target genes from Targetscan, miRWalk, miRDB and miRDIP bioinformatics websites and a total of 17 common genes were identified (Fig. 4A). We observed that 8 target genes, AMOTL2, BCL2L2, CACHD1, MSRB3, NFIB, S1PR2, SORT1 and SRF, were significantly down-regulated in lung adenocarcinoma (Fig. 4B). Results from THPA data revealed the decreased expression of those genes (Fig. 4C-J) in lung adenocarcinoma tissues.

Then we investigated the association between 8 target genes and overall survival (Fig. 5A-H). The Hazard Ratios were 0.520 (95%CI: 0.400–0.670; P = 2.700e-07), 0.650 (95%CI: 0.520–0.830; P = 3.300e-03), 0.520 (95%CI: 0.400–0.670; P = 1.700e-07), 0.440 (95%CI: 0.350–0.570; P = 4.900e-11), 0.530 (95%CI: 0.420–0.680; P = 2e-07), 0.570 (95%CI: 0.440–0.740; P = 1.500e-05), 0.520 (95%CI: 0.400–0.660; P = 1.300e-07), 0.620 (95%CI: 0.480–0.790; P = 8.900e-05), respectively. In addition, univariate and multivariate analyses indicated that the downregulation of those target genes were independent risk factors for lung adenocarcinoma survival (Fig. 5I-P).

Furthermore, we found the significant correlation between miR-149-5p and AMOTL2 (Fig. 6A: r=-0.354, P < 0.001) and MERB3 (Fig. 6D: r=-0.120, P = 0.043) in TCGA-LUAD cohort.

Discussion

Exosomal microRNAs play vital roles in the occurrence and development of tumors[8, 16, 17]. Exosomal miR-155 elevated growth rates of tumor cells in gastric carcinoma via c-MYB/VEGF axis[18]. Up-regulation of exosomal miR-146b-5p and miR-222-3p augmented migration and invasion abilities of papillary thyroid carcinomas[19]. Additionally, it was found that BMMSC-derived exosomal miR-144 suppressed growth of tumor cells and colony formation in NSCLC by targeting CCNE1 and CCNE2[20]. In colorectal cancer, overexpression of exosomal miR-106b-3p was significantly associated with poor prognosis[21]. In our study, we found that exosmal miR-149-5p was highly expressed in peripheral serum of lung adenocarcinoma patients. RT-PCR assay results further confirmed that exosomal miR-149-5p was highly expressed in A549 cells. These results validate the hypothesis that exosomal miR-149-5p may be function as an oncogene in lung adenocarcinoma. In addition, MTS and Transwell assays demonstrated that exosomal miR-149-5p stimulated proliferation and migration of tumor cells. In contrast, it inhibited

apoptosis of A549 cells. These findings point to a potential role of exosomal miR-149-5p as an alternative biomarker for lung adenocarcinoma.

To identify the downstream targets of exosomal miR-149-5p, bioinformatics tools were used to predict target genes. Among them, 8 genes were aberrantly expressed and were associated with poor survival of lung adenocarcinoma. Further, analysis of association between miR-149-5p and target genes revealed that miR-149-5p was a negative regulator of AMOTL2 and MERB3, indicating that exosomal miR-149-5p regulated metastasis of tumor cells by targeting AMOTL2 and MSRB3 genes.

The AMOT gene family members function as tumor suppressors in several human cancers. AMOT was significantly downregulated in lung cancer tissues and tumor cells[22]. Particularly, AMOTL2 played an important regulatory role in tumor microenvironment. In breast cancer, AMOTL2 increased LATS kinase activity leading to the suppression of metastasis of tumor cells[23]. Besides, when downregulated, AMOTL2 enhanced tumor cells growth[24], migration and angiogenesis[25] via Hippo pathway in hepatocellular carcinoma. MESRB3 regulates proliferation of MEF cells via enhancing the protein level of p27[26]. In breast cancer, deficiency of MSRB3 promoted tumor cells apoptosis via the intrinsic mitochondrial apoptosis pathway[27], p53-independent and ER stress-dependent pathways[28]. In addition, MSRB3 was significantly downregulated in gastric cancer and it predicted poor prognosis[29]. On the other hand, up-regulation of MSRB3 accelerated renal cell carcinoma cells metastasis[30]. However, effect of AMOTL2 and MSRB3 on lung adenocarcinoma is incompletely understood. In our study, AMOTL2 and MSRB3 were found to be tumor suppressor genes in lung adenocarcinoma. Univariate and multivariate analyses results showed the low expressions levels of AMOTL2 and MSRB3 were independent risk factors for predicting overall survival in lung adenocarcinoma. Moreover, we inferred that exosomal miR-149-5p participated in progression of tumor cells via regulating AMOTL2 and MSRB3.

Conclusion

In summary, we analyzed GSE111803 raw data and identified genes for construction of a WGCNA co-expression network. Our results demonstrated that exosomal miR-149-5p suppressed the growth, migration and apoptosis of tumor cells in lung adenocarcinoma. Aberrant expression of target genes of exosomal miR-149-5p could be independent factors for predicting the survival of lung adenocarcinoma patients. Our study suggests that exosomal miR-149-5p may be a novel tumor microenvironment biomarker in lung adenocarcinoma.

Abbreviations

BMMSC	Bone marrow mesenchymal stem cells
FBS	Fetal calf serum
GEO	Gene expression omnibus
KEGG	Kyoto encyclopedia of genes and genomes
LUAD	Lung adenocarcinoma
MEF	Mouse embryonic fibroblast
NC	Negative control
NSCLC	Non-small cell lung cancer
OD	Optical density
PBS	Phosphate buffer solution
RT-PCR	Reverse transcription-polymerase chain reaction
TCGA	The Cancer Genome Atlas
THPA	The human protein atlas
WGCNA	Weighted gene co-expression network analysis

Declarations

Ethics approval and consent to participate

Not applicable.

Consent for publication

Not applicable.

Availability of data and materials

Data and material will be available from GEO datasets (https://www.ncbi.nlm.nih.gov/geo/query/acc.cgi?acc=GSE111803).

Funding

This study was supported by Fund of National Natural Science Foundation of China (No. 81773524).

Competing interests

The authors declare that they have no competing interests.

Authors' contributions

He Yang analyzed the data from GEO and revised the manuscript. Wen Tian wrote the manuscript, performed experiments. Baosen Zhou provided the funding. All authors read and approved the final manuscript.

Acknowledgements

The authors appreciate all the participants and the patients for making contributions to this work.

References

1. Rodriguez-Canales J, Parra-Cuentas E, Wistuba II. Diagnosis and Molecular Classification of Lung Cancer. Cancer Treat Res. 2016;170:25–46.
2. Chen W, Zheng R, Baade PD, Zhang S, Zeng H, Bray F, Jemal A, Yu XQ, He J. Cancer statistics in China, 2015. CA Cancer J Clin. 2016;66:115–32.
3. Fujimoto J, Wistuba II. Current concepts on the molecular pathology of non-small cell lung carcinoma. Semin Diagn Pathol. 2014;31:306–13.
4. Fidler IJ. The pathogenesis of cancer metastasis: the 'seed and soil' hypothesis revisited. Nat Rev Cancer. 2003;3:453–8.
5. Denisenko TV, Budkevich IN, Zhivotovsky B. Cell death-based treatment of lung adenocarcinoma. Cell Death Dis. 2018;9:117.
6. Zhu E, Xie H, Dai C, Zhang L, Huang Y, Dong Z, Guo J, Su H, Ren Y, Shi P, et al. Intraoperatively measured tumor size and frozen section results should be considered jointly to predict the final pathology for lung adenocarcinoma. Mod Pathol. 2018;31:1391–9.
7. Ruivo CF, Adem B, Silva M, Melo SA. The Biology of Cancer Exosomes: Insights and New Perspectives. Cancer Res. 2017;77:6480–8.
8. Tomasetti M, Lee W, Santarelli L, Neuzil J. Exosome-derived microRNAs in cancer metabolism: possible implications in cancer diagnostics and therapy. Exp Mol Med. 2017;49:e285.

9. Hannafon BN, Ding WQ. Intercellular communication by exosome-derived microRNAs in cancer. Int J Mol Sci. 2013;14:14240–69.
10. Zhang J, Li S, Li L, Li M, Guo C, Yao J, Mi S. Exosome and exosomal microRNA: trafficking, sorting, and function. Genomics Proteomics Bioinformatics. 2015;13:17–24.
11. Milane L, Singh A, Mattheolabakis G, Suresh M, Amiji MM. Exosome mediated communication within the tumor microenvironment. J Control Release. 2015;219:278–94.
12. Singh R, Pochampally R, Watabe K, Lu Z, Mo YY. Exosome-mediated transfer of miR-10b promotes cell invasion in breast cancer. Mol Cancer. 2014;13:256.
13. Sun LP, Xu K, Cui J, Yuan DY, Zou B, Li J, Liu JL, Li KY, Meng Z, Zhang B. Cancerassociated fibroblastderived exosomal miR3825p promotes the migration and invasion of oral squamous cell carcinoma. Oncol Rep. 2019;42:1319–28.
14. Hu Y, Qin X, Yan D, Cao H, Zhou L, Fan F, Zang J, Ni J, Xu X, Sha H, et al. Genome-wide profiling of micro-RNA expression in gefitinib-resistant human lung adenocarcinoma using microarray for the identification of miR-149-5p modulation. Tumour Biol. 2017;39:1010428317691659.
15. Chen Q, Luo J, Wu C, Lu H, Cai S, Bao C, Liu D, Kong J. **The miRNA-149-5p/MyD88 axis is responsible for ursolic acid-mediated attenuation of the stemness and chemoresistance of non-small cell lung cancer cells**. 2019.
16. Sun Z, Yang S, Zhou Q, Wang G, Song J, Li Z, Zhang Z, Xu J, Xia K, Chang Y, et al. Emerging role of exosome-derived long non-coding RNAs in tumor microenvironment. Mol Cancer. 2018;17:82.
17. Qin Y, Sun R, Wu C, Wang L, Zhang C. **Exosome: A Novel Approach to Stimulate Bone Regeneration through Regulation of Osteogenesis and Angiogenesis**. *Int J Mol Sci* 2016, 17.
18. Deng T, Zhang H, Yang H, Wang H, Bai M, Sun W, Wang X, Si Y, Ning T, Zhang L, et al. Exosome miR-155 Derived from Gastric Carcinoma Promotes Angiogenesis by Targeting the c-MYB/VEGF Axis of Endothelial Cells. Mol Ther Nucleic Acids. 2020;19:1449–59.
19. Jiang K, Li G, Chen W, Song L, Wei T, Li Z, Gong R, Lei J, Shi H, Zhu J. Plasma Exosomal miR-146b-5p and miR-222-3p are Potential Biomarkers for Lymph Node Metastasis in Papillary Thyroid Carcinomas. Onco Targets Ther. 2020;13:1311–9.
20. Liang Y, Zhang D, Li L, Xin T, Zhao Y, Ma R. **Exosomal microRNA-144 from bone marrow-derived mesenchymal stem cells inhibits the progression of non-small cell lung cancer by targeting CCNE1 and CCNE2**. 2020, 11:87.
21. Liu H, Liu Y, Sun P, Leng K, Xu Y, Mei L, Han P, Zhang B, Yao K, Li C, et al. Colorectal cancer-derived exosomal miR-106b-3p promotes metastasis by down-regulating DLC-1 expression. Clin Sci (Lond). 2020;134:419–34.
22. Hsu YL, Hung JY, Chou SH, Huang MS, Tsai MJ, Lin YS, Chiang SY, Ho YW, Wu CY, Kuo PL. Angiomotin decreases lung cancer progression by sequestering oncogenic YAP/TAZ and decreasing Cyr61 expression. Oncogene. 2015;34:4056–68.
23. Kim M, Kim M, Park SJ, Lee C, Lim DS. Role of Angiomotin-like 2 mono-ubiquitination on YAP inhibition. EMBO Rep. 2016;17:64–78.

24. Jia J, Qiao Y, Pilo MG, Cigliano A, Liu X, Shao Z, Calvisi DF, Chen X. **Tankyrase inhibitors suppress hepatocellular carcinoma cell growth via modulating the Hippo cascade**. 2017, 12:e0184068.
25. Han H, Yang B, Wang W. Angiomotin-like 2 interacts with and negatively regulates AKT. Oncogene. 2017;36:4662–9.
26. Lee E, Kwak GH, Kamble K, Kim HY. Methionine sulfoxide reductase B3 deficiency inhibits cell growth through the activation of p53-p21 and p27 pathways. Arch Biochem Biophys. 2014;547:1–5.
27. Kwak GH, Kim TH, Kim HY. Down-regulation of MsrB3 induces cancer cell apoptosis through reactive oxygen species production and intrinsic mitochondrial pathway activation. Biochem Biophys Res Commun. 2017;483:468–74.
28. Kwak GH, Kim HY. MsrB3 deficiency induces cancer cell apoptosis through p53-independent and ER stress-dependent pathways. Arch Biochem Biophys. 2017;621:1–5.
29. Ma X, Wang J, Zhao M, Huang H, Wu J. Increased expression of methionine sulfoxide reductases B3 is associated with poor prognosis in gastric cancer. Oncol Lett. 2019;18:465–71.
30. Ye X, Liang T, Deng C, Li Z, Yan D. MSRB3 promotes the progression of clear cell renal cell carcinoma via regulating endoplasmic reticulum stress. Pathol Res Pract. 2020;216:152780.

Figures

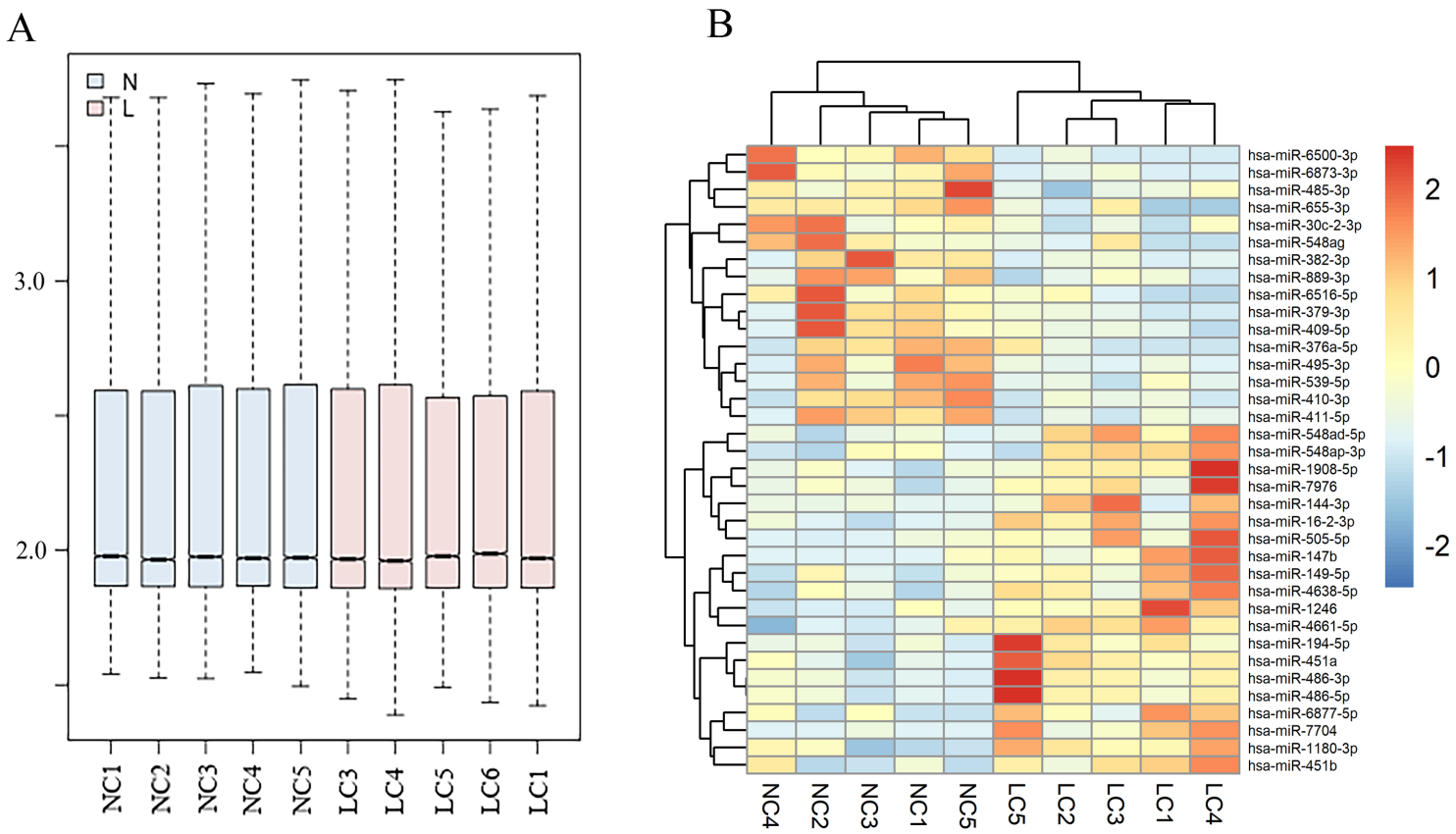

Figure 1

Differently expressed exosomal miRNAs in GSE111803. (A) Normalization of raw data in GSE111803. (B) The heat map of differently expressed exosomal miRNAs in GSE111803.

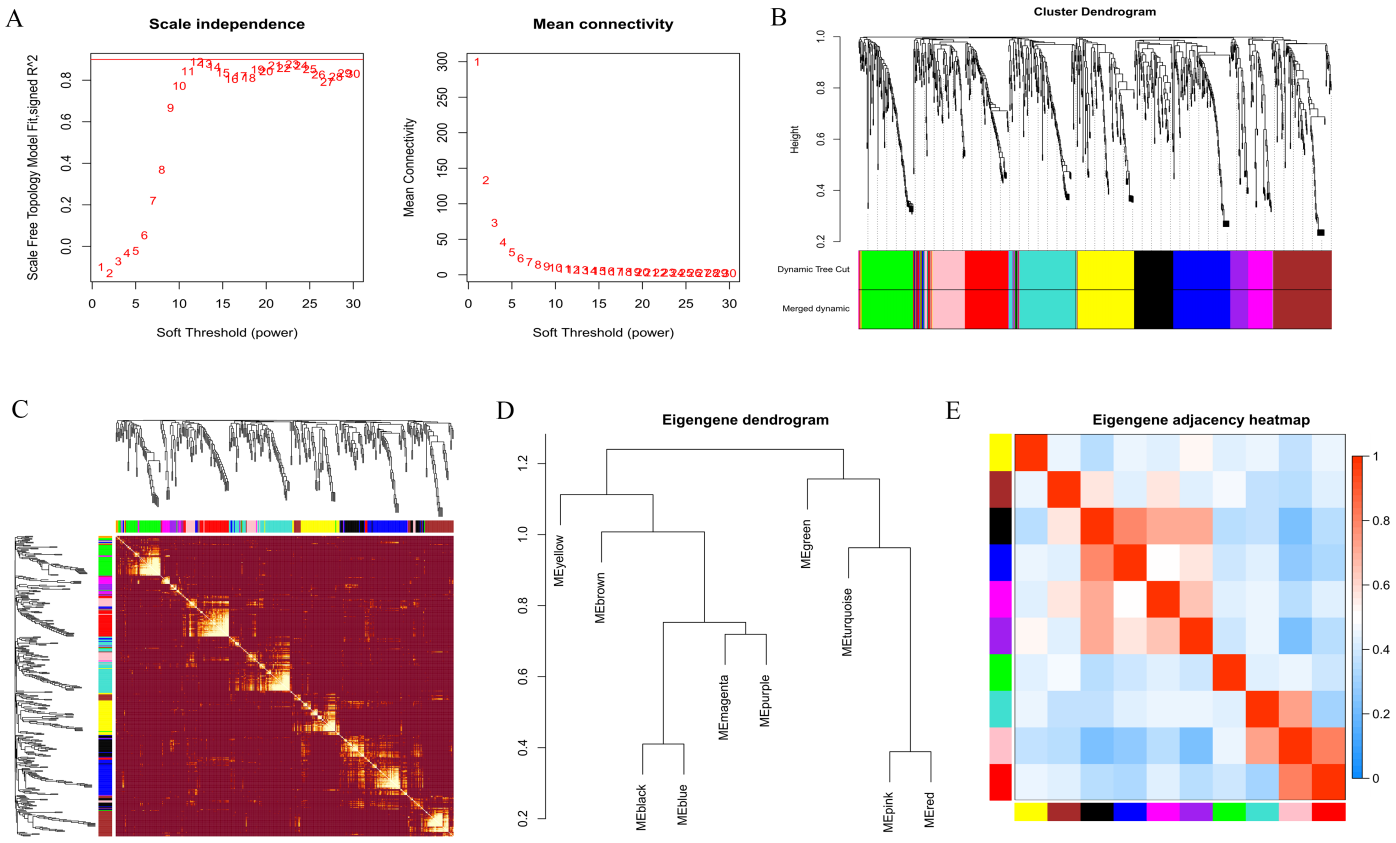

Figure 2

Construction of WGCNA. (A) Analyses of scale-free fit index and mean connectivity for various soft-thresholding powers. (B) Clustering dendrograms of exosomal miRNAs based on a dissimilarity measure. (C) The hierarchical clustering dendrograms correspond to each module. (D) Hierarchical clustering of each exosomal miRNAs module. (E) The heatmap plot of the adjacencies in the exosomal miRNAs modules.

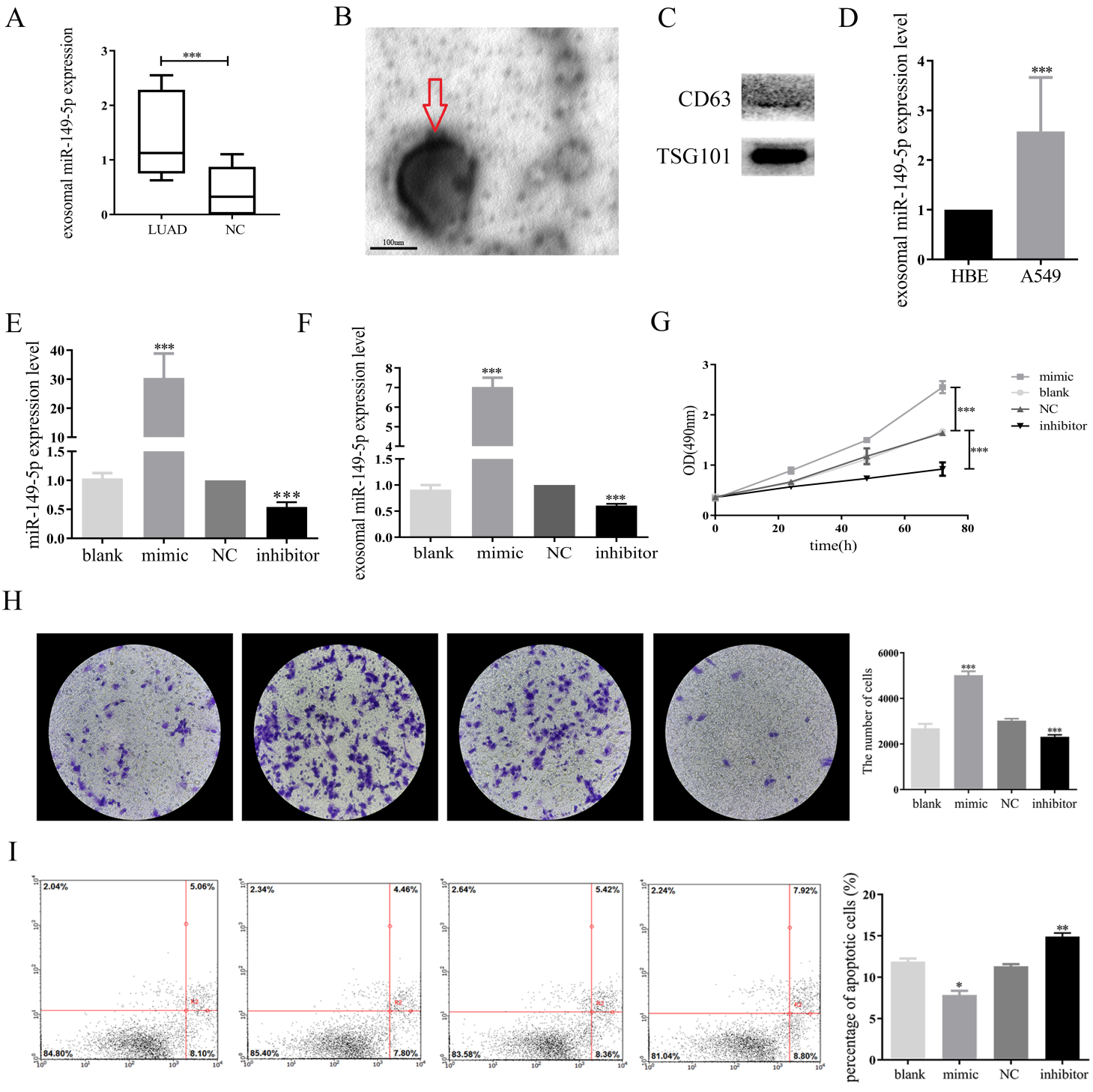

Figure 3

Exosomal miR-149-5p regulated the proliferation, migration and apoptosis of tumor cells. (A) Upregulation of exosomal miR-149-5p in lung adenocarcinoma compared to healthy controls. (B) The transmission electron micrograph of A549 cells exosomes. (C) Western blot analyses for exosomal markers, CD63 and TSG101. (D) Upregulation of exosomal miR-149-5p in A549 cells compared to HBE cells. (E) miR-149-5p expression of A549 cells with different treatments. (F) Exosomal miR-149-5p expression of A549 cells with different treatments. (G) MTS analyses of A549 cells with different

treatments. (H) Transwell analyses of A549 cells with different treatments. (I) Apoptotic rates of A549 cells with different treatments. *p<0.05, **p<0.01, ***p<0.001

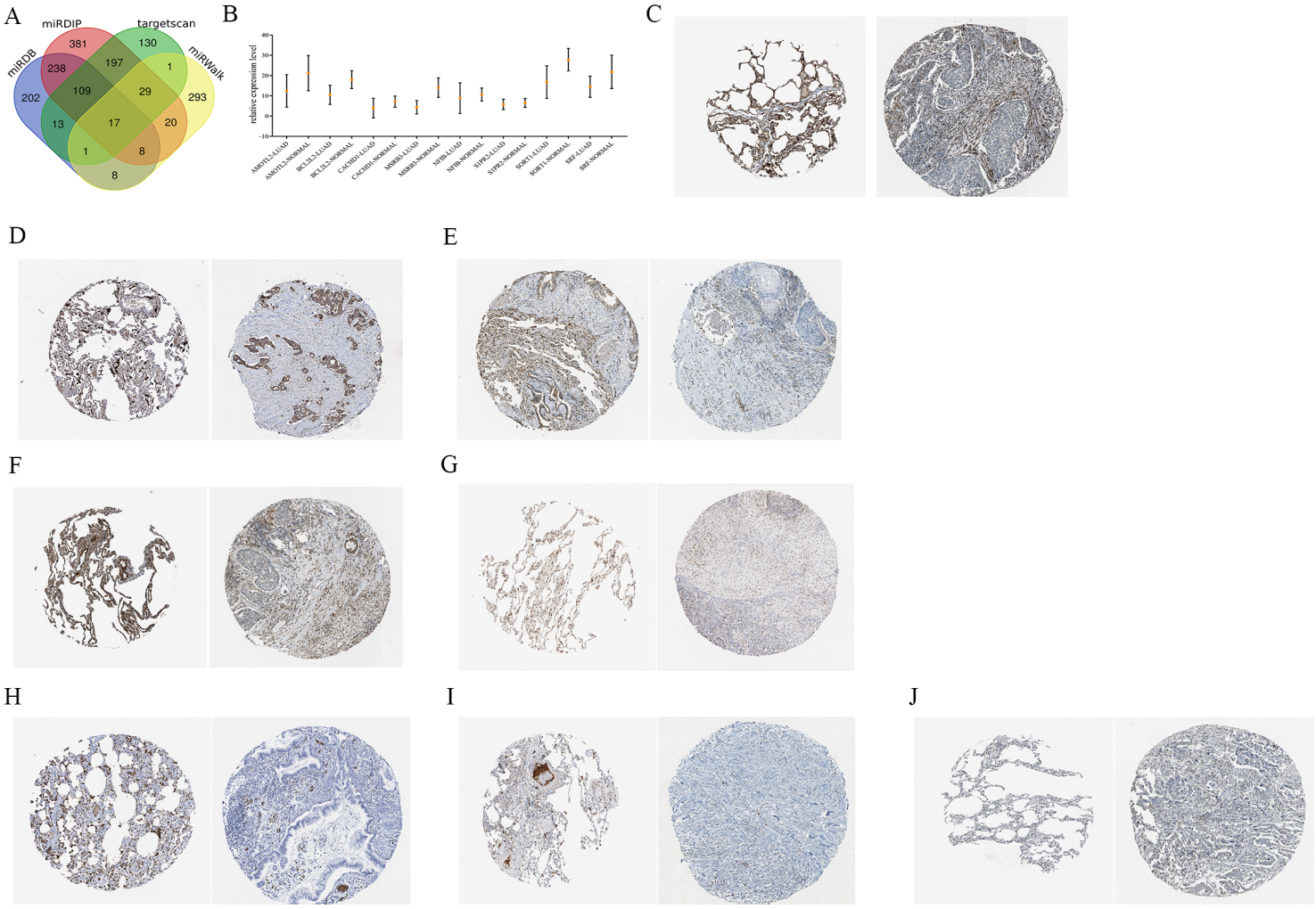

Figure 4

Expression of target genes of exosomal miR-149-5p. (A) Common target genes of exosomal miR-149-5p from targetscan, miRWalk, miRDB and miRDIP. (B) Expression profiles of target genes inTCGA-LUAD cohort. (C) Protein expression of AMOTL2 in normal tissues and lung adenocarcinoma tissues. (D) Protein expression of BCL2L2 in normal tissues and lung adenocarcinoma tissues. (E) Protein expression of CACDH1 in normal tissues and lung adenocarcinoma tissues. (F) Protein expression of MSRB3 in normal tissues and lung adenocarcinoma tissues. (G) Protein expression of NFIB in normal tissues and lung adenocarcinoma tissues. (H) Protein expression of S1PR2 in normal tissues and lung adenocarcinoma tissues. (I) Protein expression of SORT1 in normal tissues and lung adenocarcinoma tissues. (J) Protein expression of SRF in normal tissues and lung adenocarcinoma tissues.

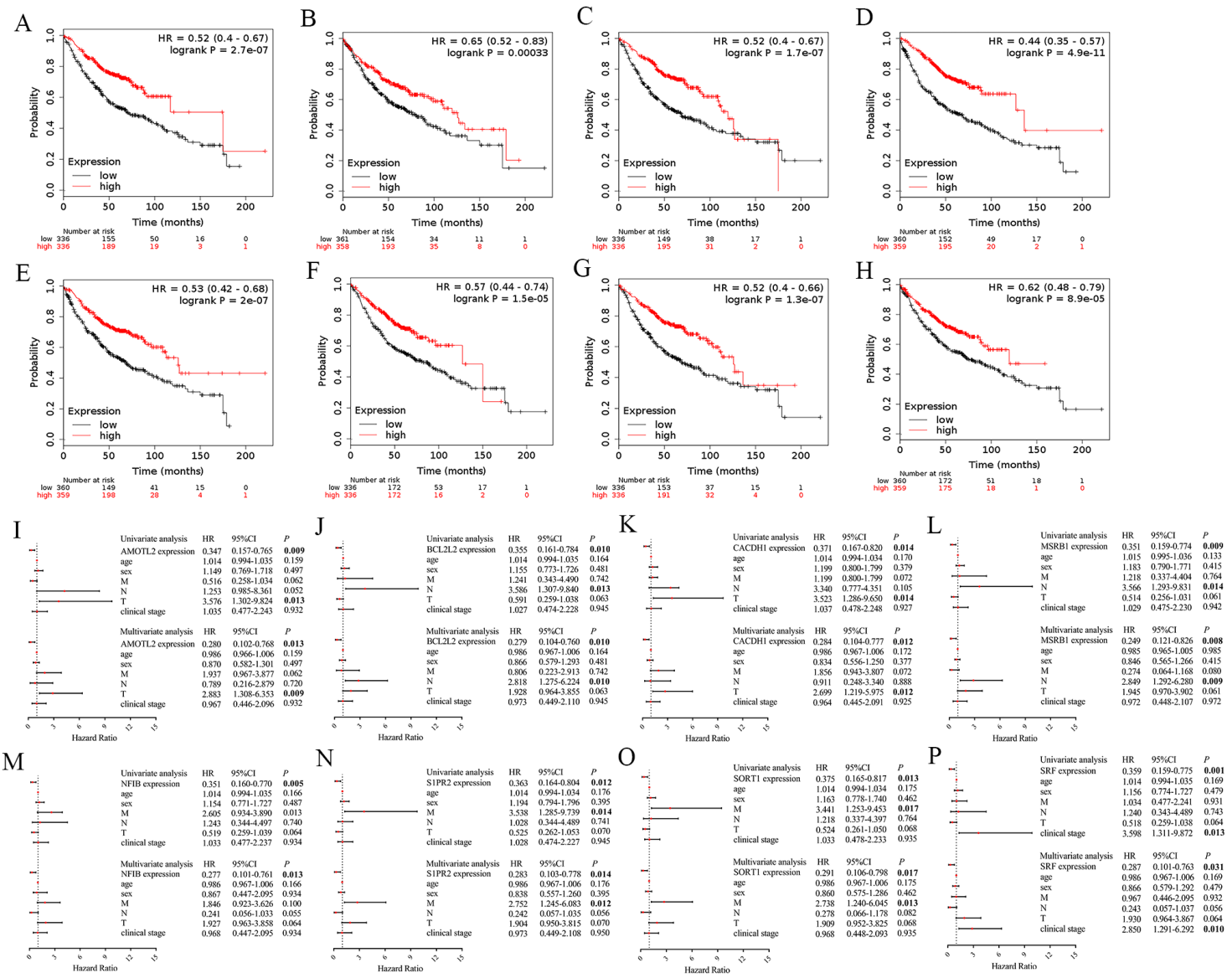

Figure 5

Integrative analyses of target genes. (A) Survival analyses of AMOTL2 in TCGA-LUAD cohort. (B) Survival analyses of BCL2L2 in TCGA-LUAD cohort. (C) Survival analyses of CACDH1 in TCGA-LUAD cohort. (D) Survival analyses of MSRB3 in TCGA-LUAD cohort. (E) Survival analyses of NFIB in TCGA-LUAD cohort. (F) Survival analyses of S1PR2 in TCGA-LUAD cohort. (G) Survival analyses of SORT1 in TCGA-LUAD cohort. (H) Survival analyses of SRF in TCGA-LUAD cohort. (I) Univariate and multivariate analyses of AMOTL2 in TCGA-LUAD cohort. (J) Univariate and multivariate analyses of BCL2L2 in TCGA-LUAD cohort. (K) Univariate and multivariate analyses of CACDH1 in TCGA-LUAD cohort. (L) Univariate and multivariate analyses of MSRB3 in TCGA-LUAD cohort. (M) Univariate and multivariate analyses of NFIB in TCGA-LUAD cohort. (N) Univariate and multivariate analyses of S1PR2 in TCGA-LUAD cohort. (O) Univariate and multivariate analyses of SORT1 in TCGA-LUAD cohort. (P) Univariate and multivariate analyses of SRF in TCGA-LUAD cohort.

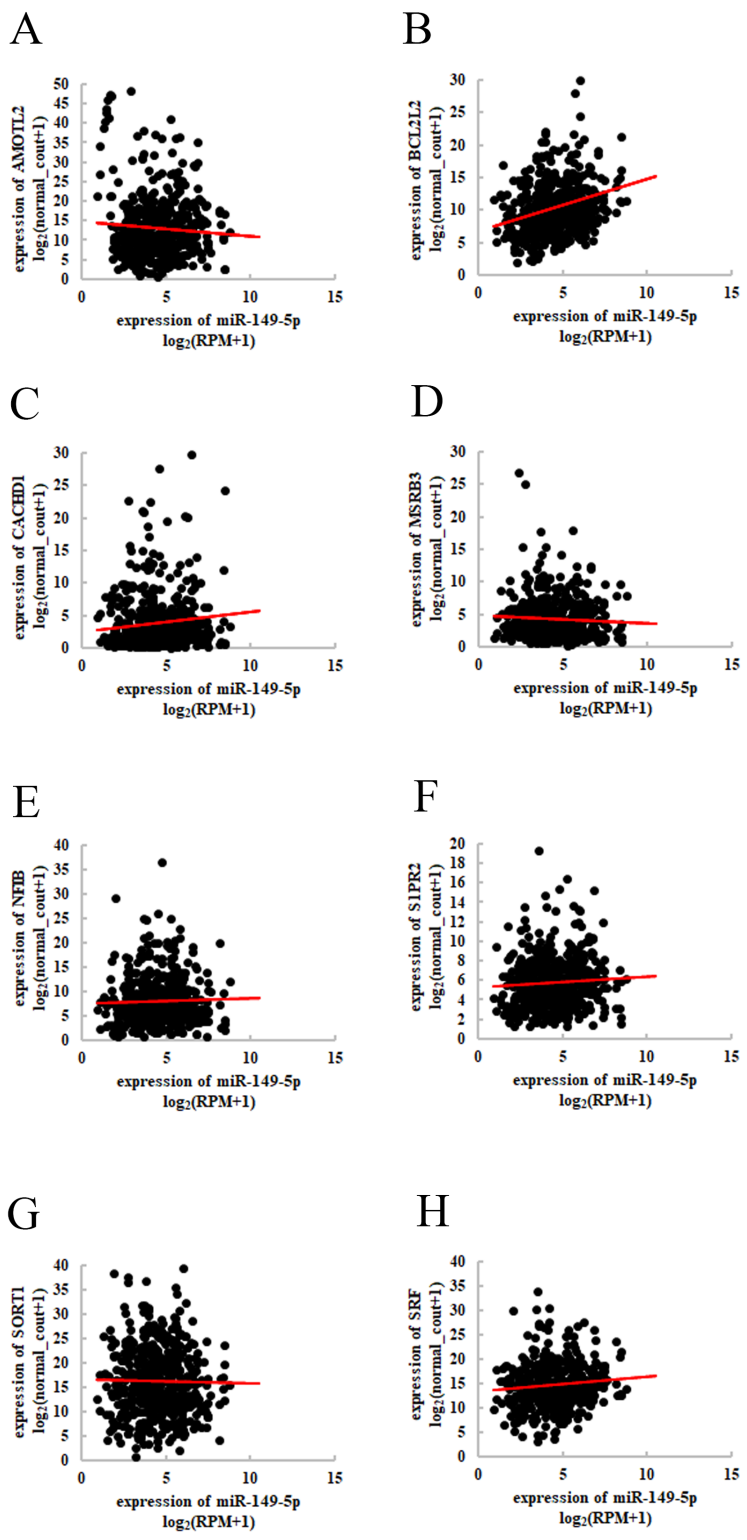

Figure 6

Correlation between target genes and miR-149-5p expression in TCGA-LUAD cohort. (A) Correlation between AMOTL2 and miR-149-5p expression in TCGA-LUAD cohort. (B) Correlation between BCL2L2 and miR-149-5p expression in TCGA-LUAD cohort. (C) Correlation between CACDH1 and miR-149-5p expression in TCGA-LUAD cohort. (D) Correlation between MSRB3 and miR-149-5p expression in TCGA-LUAD cohort. (E) Correlation between NFIB and miR-149-5p expression in TCGA-LUAD cohort. (F)

Correlation between S1PR2 and miR-149-5p expression in TCGA-LUAD cohort. (G) Correlation between SORT1 and miR-149-5p expression in TCGA-LUAD cohort. (H) Correlation between SRF and miR-149-5p expression in TCGA-LUAD cohort.